Fuel 349 (2023) 128677

Contents lists available at ScienceDirect

Fuel

journal homepage: www.elsevier.com/locate/fuel

Full Length Article

Measurement and prediction of the volumetric and acoustic properties of two biodiesel fuels up to 200 MPa

Matthieu Habrioux [a,b], Djamel Nasri [a], João A.P. Coutinho [c], Jean-Luc Daridon [a,*]

[a] Universite de Pau et des Pays de l'Adour, E2S UPPA, CNRS, TotalEnergies, Laboratoire des Fluides Complexes et Leurs Réservoirs, 64000 Pau, France
[b] present adress : CESI, 8 Rue des Frères Charles et Alcide d' Orbigny, 64000 Pau, France
[c] CICECO, ChemistryDepartment, Universityof Aveiro, Campus de Santiago, 3810 – 193 Aveiro, Portugal

ARTICLE INFO

Keywords:
Biodiesel
High pressure
Density
Speed of sound
Compressibility

ABSTRACT

This work presents experimental data on sound velocities and densities for two biodiesel fuels, namely sunflower methyl ester and a blend of Palm, Rapeseed, and Soybean methyl esters at pressures ranging from atmospheric to 200 MPa and temperatures from 293.15 to 393.15 K. Speed of sound data were obtained up to 200 MPa using a pulsed echo method. Density was determined by measuring the period of a vibrating tube up to 100 MPa and by integrating the sound velocity between 100 and 200 MPa. These measurements were coupled to determine other properties, such as isothermal compressibility, isentropic compressibility, and acoustic impedance, which strongly influence the injection process in diesel engines. The experimental data were compared with a set of models previously developed to predict the density and sound velocity of biodiesels under high pressure based on their fatty acid ester composition.

1. Introduction

In an effort to improve engine efficiency and reduce harmful diesel engine emissions, a promising approach consists of improving combustion processes by raising the injection pressure [1,2]. Additionally, the use of non-conventional fuels may help to reduce exhaust emissions without making drastic changes to the design of diesel engines. Regarding the reduction of air pollution, a very attractive alternative fuel is biodiesel fuel (B100) or biodiesel-petrodiesel blends (B5, B10, B20…). Compared to diesel from petroleum refining, diesel from biomass offers several environmental benefits. Using biodiesel instead of petrodiesel leads to a reduction in unburned fuels. This also helps to reduce emissions [3,4] of carbon monoxide, sulfur oxides, sulfates, as well as particulate matter created by incomplete combustion. On the other hand, substituting conventional petrodiesel fuel with biodiesel may, in some cases, lead to trouble in the engine function, such as deposits within the fuel system and higher NOx emissions [3,4]. However, the actual advantages and disadvantages of using biodiesel vary significantly depending on the biodiesel thermophysical properties [5–7]. These properties are directly influenced by the temperature and pressure of engine operating conditions, as well as by the composition of biodiesel in fatty acid alkyl esters, which depends on the feedstock source [8]. Consequently, to make the best possible use of biodiesel, accurate knowledge of the thermophysical properties of biodiesel is required as a function fatty acid alkyl esters composition as well as temperature and pressure.

With the aim of obtaining high-pressure volumetric properties of biodiesel fuels, regardless of the type of biomass resource and alcohol used in the transesterification reaction, we have developed [9] a method capable of predicting in an extended range of pressure (up to 200 MPa) with uncertainties comparable to experimental ones, both the density ρ and its derivatives, based solely on their fatty acid alkyl ester profiles. The proposed method was initially based on a group contribution technique to predict the molar volume of pure fatty acid alkyl esters through the simple addition of five group volume increments. Then, from the group contribution predictions, a correlation was developed to express the density in fatty acid methyl and ethyl ester components as a function of pressure and temperature using a Murnaghan-type equation [10]. Finally, a combination rule was used to extend the pure fatty acid alkyl ester correlations to the prediction of the density of biodiesel fuels from their fatty acid alkyl ester composition. This strategy, based on a combination of a group contribution method for determining pure components properties, and a combining rule for predicting mixture behavior, was consistently extended to the prediction of the speed of

* Corresponding author.
E-mail address: jean-luc.daridon@univ-pau.fr (J.-L. Daridon).

https://doi.org/10.1016/j.fuel.2023.128677
Received 13 March 2023; Received in revised form 26 April 2023; Accepted 9 May 2023

sound of biodiesels under high pressure [11]. This was achieved by considering cMγ the product of speed of sound c and molecular weight M raised to to a constant power $\gamma = 0.975$ instead of speed of sound, as this quantity proved appropriate for group additivity rules in the alkane family [12]. Both these predictive methods have been validated by comparing their predictions with experimental data from different sources and obtained with various measurement techniques [9,11]. However, while there is much data concerning density and speed of sound in biodiesel fuels under atmospheric pressure, fewer focus on the high-pressure domain. Five works [13–17] have been carried out to report consistent densities in biodiesels beyond 100 MPa and the situation is even worse for acoustic properties, for which there has only been one article [13] published to provide data of speed of sound in biodiesels up to 200 MPa. This latter concerns only two raw materials: soybean and rapeseed oils.

Therefore, the aim of this work is to provide additional high pressure data to validate the predictive approaches against an expanded dataset concerning both volumetric and acoustic properties. Two biodiesels were investigated up to 200 MPa here; the first was obtained by transesterification of sunflower seed oil with methanol, and the second corresponded to a blend of Palm methyl ester, Rapeseed methyl ester and Soybean methyl ester. The speed of sound was measured for temperatures ranging from 293.15 to 393.15 K and from atmospheric pressure to 200 MPa using a pulse-echo technique. Density was determined by using a vibrating U-tube densimeter up to 100 MPa and by integrating the speed of sound between 100 and 200 MPa. By deriving and combining acoustic and volumetric data, related thermophysical properties (i.e., isothermal compressibility, isentropic compressibility and acoustic impedance Z) of biodiesel fuels were estimated. All these derivative properties, in addition to speed of sound and density, were compared to the predictions of the predictive methods developed previously [9,11].

2. Experimental measurements

2.1. Materials

The biodiesels were prepared by transesterification of four different vegetable oils (sunflower seed, palm, rapeseed and soybean) with methanol (Sigma, mole fraction purity 0.999). For each oil, the ratio (in mol) between oil and alcohol was set at 1:5 to ensure the completion of the reaction. The transesterification was carried out at 328.15 K using sodium hydroxide as a catalyst. At the end of the reaction, the obtained product was washed to eliminate the remaining alcohol, catalyst, and glycerol produced by the reaction. Finally, the obtained biodiesel was dried by contacting it with anhydrous sodium sulfate until a water content of less than 0.05 wt% was reached. This water content limit was verified through Karl-Fischer titration. The sunflower seed oil biodiesel sample (MB-SF) was investigated pure, while the other samples were mixed in equimass proportion to obtain a Palm-Rapeseed-Soybean biodiesel blend (MB-PRS). The detailed fatty acid methyl ester (FAME) profile between methyl-caprate (C10:0) and methyl-lignocerate (C24:0) of both these biodiesels are given in mole % in Table 1, wherein the Cm:n symbol refers to the carbon chain length (m) and number of double bonds (n) of the related fatty acid. These compositions were determined using gas chromatography with flame ionization detection (GC-FID), following the British Standard EN 14103 from EN 142144 [18]. A Varian CP-3800 with a FID in a split injection system with a select biodiesel for FAME column (30 m 0.32 mm 0.25 μm) was used to discriminate between all methyl esters in analysis, including the polyunsaturated ones. The column temperature was set at 120 °C and then programmed to increase up to 250 °C at 4 °C/min. The detector and injector were set at 250 °C. The carrier gas was helium with a flow rate of 2 mL/min.

Table 1
Fatty Acid Methyl Ester profiles in mol% of biodiesels studied.

FAME	MB-SF	MB-PRS
C10:0	0.00	0.02
C12:0	0.03	0.19
C14:0	0.08	0.46
C16:0	6.95	20.40
C16:1	0.10	0.15
C18:0	4.15	3.20
C18:1	23.68	41.71
C18:2	64.02	27.59
C18:3	0.12	4.63
C20:0	0.03	0.40
C20:1	0.14	0.47
C22:0	0.63	0.27
C22:1	0.07	0.11
C24:0	0.00	0.40

2.2. Speed of sound measurement

The speed of sound was measured up to 200 MPa using a fixed-path-length pulse-echo technique. The apparatus mainly consists of an immersion ultrasonic sensor housed in a high-pressure cell closed by a plug with three high-pressure electrical feedthroughs used to connect the sensor to a high-voltage pulse generator. A detailed description of the ultrasonic sensor is given in a previous paper [19]. It is mainly formed by two longitudinal ultrasonic wave transducers housed at both ends of a hollow stainless steel cylinder and placed one in front of the other at a distance L corresponding to the path length of the wave through the fluid. This acoustic path length was calibrated with water [20,21] and checked by carrying out experiments in pure n-heptane [22,23] prior to the measurements.

The speed of sound was determined by a time-of-flight method that consists of generating a short, high-frequency (3 MHz) sound pulse using the first transducer (transmitter) and measuring the time delay between two successive echoes received by the second transducer (receiver) using a digital overlap method presented in detail in a previous paper [24].

To stabilise the temperature of sample during isothermal measurements, the pressure cell was completely immersed in a thermostatic bath filled with a heat-carrying liquid, and the temperature was directly measured in the fluid by a platinum probe (Pt100) that was pressure-protected by a metal finger. With this arrangement, the temperature of the sample fluid was measured with a standard uncertainty of $u(T) = 0.1$K. The studied fluid was pressurised by means of an external volumetric pump. Two pressure probes were placed between the pump and the cell to allow the pressure to be measured. The first one operated within the limited range of 0–100 MPa, with a standard uncertainty of $u(p) = 0.01$ MPa, while the second one was used across the whole experimental range (0–200 MPa) but with a standard uncertainty of u $(p) = 0.1$ MPa. Consequently, the combined uncertainty in the speed of sound measurement was estimated to be $U(C) = 0.2\%$ between (0.1 and 100) MPa and $U(C) = 0.3\%$ between (100 and 200) MPa according with the Guide to the Expression of Uncertainty in Measurement [25].

2.3. Density measurement up to 100 MPa

Density was measured up to 100 MPa in a high-pressure vibrating-tube density meter (DMA HPM) using the oscillating U-tube principle, which relates fluid density ρ to the measurement of the vibration period τ_{fluid} of the tube containing the fluid. The pressure of the fluid in the vibrating tube was generated by a volumetric pump, and its value was monitored with a standard uncertainty of u(p) = 0.1 MPa, thanks to a pressure gauge located between the pump and density meter. The temperature of the high pressure U-tube was controlled by the circulation of a heat carrier liquid connected to a thermostatic circulation bath and measured by a platinum probe with a standard uncertainty of $u(T) = 0.1$K. The periods of vibration were converted into density by means of the physically-based model proposed by May et al. [26] to represent the resonance behavior of a U-tube filled with a high pressure fluid. The following working equation was applied:

$$\rho(T,p) = \frac{A_0(1+\beta_\tau p)}{\left(1+\varepsilon_1(T-T_0)+\varepsilon_2(T-T_0)^2\right)^2(1+\alpha_V(T-T_0)+\beta_V p)}\tau_{fluid}^2 - \frac{B_0}{(1+\alpha_V(T-T_0)+\beta_V p)} \quad (1)$$

where A_0, B_0, β_τ, β_V, α_V, ε_1 and ε_2 are seven instrument parameters related to the characteristics of the oscillating tube. These parameters were estimated by calibration with both vacuum and water over the same p,T ranges as those of measurements carried out in biodiesels. The density of water obtained from IAWPS equation of state [27] was considered for this calibration. Taking into account the uncertainties of these reference densities, as well as the uncertainties in the measurement of temperature, pressure, and periods of vibration, the expanded uncertainty associated with the reported densities was estimated by a Monte Carlo method to be $U(\rho) = 1\text{kg}\cdot\text{m}^{-3}$ according to the guide to the expression of uncertainty in measurement [28].

2.4. Density determination between 100 and 200 MPa

To cover the same high-pressure range for both density and speed of sound data, the density data was extended from 100 to 200 MPa by integrating speed of sound data. The method used to get high-pressure density from sound velocity is identical to one previously described [29]. It's based on the relationship between isentropic κ_S and isothermal κ_T compressibilities and the Newton-Laplace relation, which connects speed of sound c to isentropic compressibility. By combining and integrating these relationships, density change with pressure is related to speed of sound according to the following equation:

$$\rho(p,T) - \rho(p_{ref},T) = \int_{p_{ref}}^{p} \frac{1}{c^2}dp + T\int_{p_0}^{p} \frac{\alpha_P^2}{c_P}dp \quad (2)$$

where α_P is the isobaric thermal expansion and c_P the isobaric specific heat capacity.

The first term on the right side of Eq. (2) is the main contributor to the change in density with respect to pressure. It was calculated by first fitting a 2D smoothing function to sound speed data and then performing an analytical integration of this function. For this purpose, the rational function previously proposed by Ndiaye et al. [19] to correlate speed of sound of pure fatty acid methyl esters was utilized. It has the following form and requires 9 parameters:

$$\frac{1}{c^2} = \frac{A + B_1T + B_2T^2 + B_3T^3 + C_1p + C_2p^2 + C_3p^3}{1 + ET + Fp} \quad (3)$$

The second term on the right side of Eq. (2) was calculated numerically using a predictor–corrector method presented in detail in a previous publication [29]. During the iteration process, the heat capacity in Eq. (2) is estimated together with the density using the following integrated thermodynamic relation:

$$c_p(p,T) - c_p(p_{ref},T) = \int_{p_{ref}}^{p} -\frac{T}{\rho}\left(\alpha_p^2 + \left(\frac{\partial \alpha_p}{\partial T}\right)_p\right)dp \quad (4)$$

The isobaric thermal expansion and its derivative involved in this equation as well as in Eq. (2) are computed at each iteration by fitting a polynomial function to isobaric density values and differentiating it. Further informations on the predictor–corrector algorithm can be found in a previous paper [29].

The determination of $\rho(p,T)$ and $c_p(p,T)$ from Eqs. (2) and (4) requires their values to be known at an initial pressure p_{ref}. This pressure was chosen as $p_{ref} = 100$ MPa so that the input values for the density $\rho(p_{ref},T)$ were directly taken from vibrating-tube density meter measurements and correlated with temperature using a polynomial function. To determine the initial heat capacities $c_p(p_{ref},T)$ measurements were first conducted at atmospheric pressure p_{atm} using a differential scanning calorimeter that operates in continuous mode with a constant heating rate of 0.2 K min^{-1}. The atmospheric heat capacities values $c_{p0}(T)$ were then extended to p_{ref} by numerically integrating Eqs. (2) and (4) between p_{atm} and p_{ref}. The results were then correlated using a second-order polynomial function. The parameters of the correlations for both $\rho(p_{ref},T)$ and $c_p(p_{ref},T)$ along with the coefficients of Eq. (3) are used as input for the thermodynamic integration. This allows the choice of grid size for the numerical procedure for both temperature derivation and pressure integration. A grid size of 1 K and 0.1 MPa was chosen here for temperature and pressure steps, respectively. The uncertainty in the densities calculated from this numerical integration was determined using a Monte Carlo method, in which each input data is replaced by a discrete pseudorandom distribution with a standard deviation equal to its standard uncertainty.

3. Results and discussion

3.1. Experimental results

For both biodiesels, the speed of sound was measured along 6 isotherms ranging from 293.15 to 393.15 K at pressures up to 200 MPa, in steps of 10 MPa up to 100 MPa, and of 20 MPa above that pressure. The lower pressure of the investigated isotherms was either 0.1 MPa or 10 MPa when the vapor pressure was higher than the atmospheric pressure. The measurement results are listed in Table 2. In order to integrate speed of sound data between 0.1 and 100 MPa and then between 100 and 200 MPa, the square of the speed of sound was correlated with temperature and pressure using Eq. (3) in both of these pressure ranges separately. The coefficients for both sets were reported in Table 3 for each biodiesel, alongside the Mean Percentage Deviation (MPD), Mean Absolute Percentage Deviation (MAPD), and the Maximum Percentage Deviation (MaxPD) from the experimental data. These statistics show that the chosen rational form leads to a good fit of the speed of sound data with a maximum deviation lower than the experimental uncertainty for both biodiesels.

The density was measured with the vibrating tube densimeter up to 100 MPa in the temperature range of 293.15–393.15 K, using a temperature increment of 10 K. This increment was reduced compared to the one considered for speed of sound measurements in order to provide a finer representation of the influence of temperature on density and thus improve the estimation of its derivative with respect to temperature. Density determination was then extended from 100 to 200 MPa, based on Eqs. (2) and (4) integrated iteratively as presented in the previous section.

The isobaric specific heat capacity $c_{p0}(T)$ required to initiate the thermodynamic integration of speed of sound was measured continuously from 293.15 to 393.15 K and at atmospheric pressure. The results were correlated in terms of the following second order polynomials:

$$\frac{c_{p0}}{(J.K^{-1}.kg^{-1})} = 1.438\times10^3 + 8.289\times10^{-1}\frac{T}{K} + 3.260\times10^{-3}\left(\frac{T}{K}\right)^2 \text{for MB}-\text{SF} \quad (5)$$

$$c_{p0}/(J.K^{-1}.kg^{-1}) = 1.509\times10^3 + 6.439\times10^{-1}\,T/K + 3.467\times10^{-3}\,(T/K)^2 \text{ for MB-PRS} \quad (6)$$

All the density values obtained for both biodiesels between 0.1 and 200 MPa are reported in Table 4. The determination of density from speed of sound is based on the integration of compressibility with respect to pressure, and thus the method also provides the isothermal

Table 2
Experimental values of speed of sound c at temperatures T and pressure[a]s p for biodiesels MB-SF and MB-PRS [a].

P/MPa	T/K	c/m s^{-1}	T/K	c/m s^{-1}	T/K	c/m s^{-1}
	MB-SF					
0.1	293.15	1415.1	313.15	1342.5	333.15	1275.7
10	293.15	1458.2	313.15	1389.9	333.15	1326.4
20	293.15	1498.7	313.15	1433.6	333.15	1374.9
30	293.15	1538.5	313.15	1474.4	333.15	1417.8
40	293.15	1575.6	313.15	1514.3	333.15	1458.4
50	293.15	1610.2	313.15	1551.3	333.15	1498.0
60	293.15	1644.6	313.15	1585.8	333.15	1534.9
70	293.15	1677.1	313.15	1619.9	333.15	1570.6
80	293.15	1706.7	313.15	1651.8	333.15	1603.6
90	293.15	1737.3	313.15	1683.7	333.15	1636.6
100	293.15	1764.8	313.15	1712.6	333.15	1666.8
120	–	–	313.15	1769.7	333.15	1726.6
140	–	–	313.15	1822.2	333.15	1780.3
160	–	–	313.15	1873.0	333.15	1832.7
180	–	–	313.15	1920.6	333.15	1880.3
200	–	–	313.15	1965.2	333.15	1929.0
0.1	353.15	1211.2	–	–	–	–
10	353.15	1262.9	373.15	1202.4	393.15	1144.1
20	353.15	1313.0	373.15	1255.8	393.15	1201.2
30	353.15	1360.5	373.15	1306.4	393.15	1251.7
40	353.15	1402.4	373.15	1351.0	393.15	1300.5
50	353.15	1444.1	373.15	1392.9	393.15	1344.0
60	353.15	1482.2	373.15	1432.0	393.15	1386.2
70	353.15	1519.7	373.15	1471.4	393.15	1425.0
80	353.15	1554.0	373.15	1507.0	393.15	1462.6
90	353.15	1588.9	373.15	1541.2	393.15	1498.1
100	353.15	1620.6	373.15	1574.3	393.15	1531.8
120	353.15	1680.3	373.15	1637.0	393.15	1593.9
140	353.15	1735.6	373.15	1693.7	393.15	1654.4
160	353.15	1789.4	373.15	1748.7	393.15	1710.7
180	353.15	1839.0	373.15	1797.4	393.15	1760.7
200	353.15	1887.2	373.15	1848.1	393.15	1811.1
	MB-PRS					
0.1	293.15	1409.9	313.15	1338.1	333.15	1271.4
10	293.15	1453.3	313.15	1386.3	333.15	1324.0
20	293.15	1495.6	313.15	1430.7	333.15	1371.3
30	293.15	1533.7	313.15	1473.3	333.15	1415.1
40	293.15	1571.7	313.15	1511.2	333.15	1457.4
50	293.15	1606.7	313.15	1548.3	333.15	1495.7
60	293.15	1641.4	313.15	1584.0	333.15	1533.9
70	293.15	1673.4	313.15	1617.5	333.15	1569.3
80	293.15	1703.4	313.15	1650.3	333.15	1602.3
90	293.15	1733.7	313.15	1681.2	333.15	1635.2
100	293.15	1761.4	313.15	1711.6	333.15	1666.0
120	–	–	313.15	1769.1	333.15	1725.5
140	–	–	313.15	1821.3	333.15	1780.6
160	–	–	313.15	1872.2	333.15	1832.3
180	–	–	313.15	1919.1	333.15	1883.5
200	–	–	313.15	1963.7	333.15	1929.3
0.1	353.15	1204.7	–	–	–	–
10	353.15	1259.6	373.15	1198.8	–	–
20	353.15	1310.8	373.15	1252.5	393.15	1197.6
30	353.15	1358.2	373.15	1300.6	393.15	1249.1
40	353.15	1401.6	373.15	1347.3	393.15	1297.0
50	353.15	1443.0	373.15	1391.4	393.15	1342.0
60	353.15	1481.3	373.15	1430.9	393.15	1383.9
70	353.15	1517.3	373.15	1469.2	393.15	1422.4
80	353.15	1553.1	373.15	1505.5	393.15	1461.0
90	353.15	1586.3	373.15	1540.0	393.15	1495.9
100	353.15	1615.8	373.15	1573.2	393.15	1530.5
120	353.15	1678.0	373.15	1633.4	393.15	1595.5
140	353.15	1736.1	373.15	1692.5	393.15	1653.8
160	353.15	1790.3	373.15	1749.0	393.15	1709.8
180	353.15	1840.2	373.15	1800.8	393.15	1763.9
200	353.15	1886.1	373.15	1848.6	393.15	1810.3

[a] Standard uncertainties u are u(T) = 0.1 K, u(p) = 0.01 MPa up to 100 MPa, u (p) = 0.1 MPa between (100 and 210) MPa and the combined expanded uncertainties U (level of confidence = 0.95) are U(c) = 0.002c up to 100 MPa, U(c) = 0.003c between (100 and 200).

Table 3
Parameters of Eq. (3) for biodiesels MB-SF and MB-PRS in temperature range 293.15–393.15 K and two pressure ranges 0.1–100 MPa and 100–200 MPa.

Parameters	MB-SF		MB-PRS	
	0.1–100 MPa	100–200 MPa	0.1–100 MPa	100–200 MPa
A	1.82844×10^{-08}	-9.17160×10^{-08}	2.24638×10^{-07}	2.144140×10^{-06}
B_1	1.19793×10^{-09}	2.64561×10^{-09}	-5.61340×10^{-10}	$-2.387700 \times 10^{-08}$
B_2	-1.48260×10^{-12}	-6.65670×10^{-12}	3.50055×10^{-12}	8.226670×10^{-11}
B_3	8.66804×10^{-16}	5.56509×10^{-15}	-3.58890×10^{-15}	−6.929600 × 10–14
C_1	1.25125×10^{-09}	-2.80300×10^{-10}	1.45938×10^{-09}	2.702610×10^{-08}
C_2	-4.21620×10^{-12}	1.66811×10^{-12}	-4.97880×10^{-12}	$-8.651200 \times 10^{-11}$
C_3	1.19102×10^{-14}	-2.77470×10^{-15}	1.36525 × 10-^{14}	1.389600 × 10–13
E	-1.61150×10^{-03}	-1.69212×10^{-03}	-1.57989×10^{-03}	4.145810×10^{-07}
F	5.90269×10^{-03}	2.36441×10^{-03}	6.43264×10^{-03}	6.579720×10^{-02}
Statistics				
MPD	5.9×10^{-05}	1.3×10^{-04}	-4.2×10^{-04}	1.4×10^{-03}
MAPD	5.1×10^{-02}	6.3×10^{-02}	4.8×10^{-02}	6.2×10^{-02}
MaxPD	1.4×10^{-01}	1.7×10^{-01}	1.3×10^{-01}	1.4×10^{-01}

compressibility according to the following relation:

$$\kappa_T = \frac{1}{\rho c^2} + \frac{T\alpha_P^2}{\rho c_P} \tag{7}$$

The values obtained from this equation were reported in Table S1 in the Supplementary Information file. Ultimately, the simultaneous knowledge of density and speed of sound allows the calculation of two acoustic properties that influence the injection process in diesel engines: the isentropic compressibility κ_S and acoustic impedance Z. They were determined according to the following relationships:

$$\kappa_S = \frac{1}{\rho c^2} \tag{8}$$

$$Z = \rho c \tag{9}$$

All the derived acoustic properties are provided in Tables S2 and S3 in the Supplementary Information file.

The density of biodiesel MB-PRS was previously studied by Pratas et al. [30], but only in a limited temperature range (293.15–333.15) K and up to 45 MPa. The relative deviations between the present measurements and the data provided by Pratas et al. do not exceed 0.07%, with a MAPD of 0.05% in their full working pressure–temperature range. Regarding the sunflower biodiesel, density data are available only at atmospheric pressure [31]. A comparison of these atmospheric data shows a good match, with MAPD of 0.15% and MaxPD of 0.25% for MB-SF and MB-PRS respectively. In terms of the speed of sound, high pressure values are nonexistent for both biodiesels in the literature but some data were reported by Freitas et al. [32] under atmospheric pressure for temperatures ranging from 288.15 to 343.15 K. A comparison of the present data with these measurements reveals a very good agreement, with MaxPD of 0.08 and 0.1 % for MB-SF and MB-PRS respectively.

3.2. Predictions

The measurements were conducted on both biodiesels to generate a large set of experimental data under high pressure, with the aim of testing the ability of recently developed methods [9,11] to predict the density and its derivative with respect to pressure as well as speed of

Table 4
Values of densities ρ at temperatures *T* and pressures *p* measured in liquid biodiesels MB-SF and MB-PRS by using u-tube density meter up to 100 MPa and speed of sound integration between 100 and 200 MPa.[a]

P/MPa	T/K	ρ/kg.m^{-3}	T/K	ρ/kg.m^{-3}	T/K	ρ/kg.m^{-3}	T/K	ρ/kg.m^{-3}	T/K	ρ/kg.m^{-3}	T/K	ρ/kg.m^{-3}
	MB-SF											
0.1	293.15	882.6	303.15	875.8	313.15	868.3	323.15	860.5	333.15	852.9	343.15	845.6
10	293.15	888.6	303.15	881.6	313.15	874.5	323.15	867.3	333.15	860.1	343.15	852.9
20	293.15	894.3	303.15	887.5	313.15	880.6	323.15	873.5	333.15	866.6	343.15	859.7
30	293.15	899.4	303.15	893.2	313.15	886.3	323.15	879.5	333.15	872.8	343.15	866.5
40	293.15	904.3	303.15	898.0	313.15	891.4	323.15	885.1	333.15	878.8	343.15	872.3
50	293.15	908.9	303.15	902.7	313.15	896.6	323.15	890.2	333.15	883.9	343.15	877.6
60	293.15	913.6	303.15	907.5	313.15	901.3	323.15	895.3	333.15	889.0	343.15	883.2
70	293.15	918.0	303.15	912.3	313.15	905.9	323.15	900.3	333.15	893.9	343.15	888.2
80	293.15	921.9	303.15	916.3	313.15	910.6	323.15	904.4	333.15	898.7	343.15	892.8
90	293.15	925.9	303.15	920.3	313.15	914.5	323.15	908.8	333.15	903.3	343.15	897.7
100	293.15	929.8	303.15	924.4	313.15	918.7	323.15	913.2	333.15	907.6	343.15	902.1
120	–	–	303.15	931.8	313.15	926.4	323.15	921.1	333.15	915.7	343.15	910.5
140	–	–	303.15	938.9	313.15	933.7	323.15	928.5	333.15	923.3	343.15	918.2
160	–	–	303.15	945.6	313.15	940.5	323.15	935.4	333.15	930.4	343.15	925.5
180	–	–	303.15	951.9	313.15	947.0	323.15	942.1	333.15	937.2	343.15	932.3
200	–	–	303.15	957.9	313.15	953.1	323.15	948.3	333.15	943.6	343.15	938.8
0.1	353.15	837.9	363.15	830.6	373.15	–	–	–	–	–		
10	353.15	845.9	363.15	839.3	373.15	831.9	383.15	823.6	393.15	817.4		
20	353.15	853.0	363.15	846.2	373.15	839.9	383.15	832.3	393.15	826.1		
30	353.15	859.8	363.15	853.6	373.15	847.3	383.15	839.9	393.15	834.3		
40	353.15	865.8	363.15	860.2	373.15	853.8	383.15	846.9	393.15	841.7		
50	353.15	871.8	363.15	866.1	373.15	860.1	383.15	853.4	393.15	848.4		
60	353.15	877.1	363.15	871.9	373.15	866.0	383.15	859.5	393.15	854.7		
70	353.15	882.4	363.15	877.2	373.15	871.6	383.15	865.2	393.15	860.5		
80	353.15	887.6	363.15	882.2	373.15	877.2	383.15	871.0	393.15	866.3		
90	353.15	892.2	363.15	887.1	373.15	882.0	383.15	876.1	393.15	871.5		
100	353.15	896.7	363.15	891.7	373.15	886.9	383.15	881.0	393.15	876.8		
120	353.15	905.3	363.15	900.2	373.15	895.3	383.15	890.4	393.15	885.8		
140	353.15	913.2	363.15	908.2	373.15	903.4	383.15	898.7	393.15	894.2		
160	353.15	920.6	363.15	915.8	373.15	911.1	383.15	906.5	393.15	902.1		
180	353.15	927.5	363.15	922.8	373.15	918.2	383.15	913.8	393.15	909.5		
200	353.15	934.2	363.15	929.5	373.15	925.0	383.15	920.7	393.15	916.4		
	MB-PRS											
0.1	293.15	881.6	303.15	874.3	313.15	866.8	323.15	859.6	333.15	851.9	343.15	844.6
10	293.15	887.4	303.15	880.2	313.15	873.2	323.15	866.0	333.15	858.9	343.15	851.9
20	293.15	892.7	303.15	885.9	313.15	879.0	323.15	872.1	333.15	865.2	343.15	858.5
30	293.15	897.8	303.15	891.1	313.15	884.7	323.15	877.9	333.15	871.3	343.15	864.7
40	293.15	902.7	303.15	896.2	313.15	889.9	323.15	883.3	333.15	876.8	343.15	870.6
50	293.15	907.2	303.15	901.0	313.15	894.8	323.15	888.5	333.15	882.2	343.15	876.0
60	293.15	912.1	303.15	905.5	313.15	899.5	323.15	893.3	333.15	887.3	343.15	881.4
70	293.15	915.9	303.15	909.9	313.15	904.0	323.15	898.0	333.15	892.0	343.15	886.2
80	293.15	919.9	303.15	914.1	313.15	908.4	323.15	902.5	333.15	896.5	343.15	891.0
90	293.15	923.8	303.15	918.1	313.15	912.5	323.15	906.8	333.15	901.0	343.15	895.6
100	293.15	927.7	303.15	922.2	313.15	916.5	323.15	910.9	333.15	905.4	343.15	900.0
120	–	–	303.15	929.6	313.15	924.2	323.15	918.8	333.15	913.5	343.15	908.3
140	–	–	303.15	936.7	313.15	931.4	323.15	926.2	333.15	921.0	343.15	916.0
160	–	–	303.15	943.4	313.15	938.2	323.15	933.1	333.15	928.1	343.15	923.2
180	–	–	303.15	949.8	313.15	944.7	323.15	939.7	333.15	934.8	343.15	930.0
200	–	–	303.15	955.8	313.15	950.9	323.15	946.0	333.15	941.2	343.15	936.4
0.1	353.15	837.3	363.15	830.2	–	–	–	–	–	–		
10	353.15	844.8	363.15	838.1	373.15	831.2	383.15	824.8	–	–		
20	353.15	852.0	363.15	845.4	373.15	838.7	383.15	832.6	393.15	826.2		
30	353.15	858.4	363.15	852.1	373.15	845.9	383.15	840.2	393.15	833.8		
40	353.15	864.5	363.15	858.5	373.15	852.3	383.15	846.8	393.15	841.0		
50	353.15	870.1	363.15	864.4	373.15	858.5	383.15	853.0	393.15	847.5		
60	353.15	875.5	363.15	869.6	373.15	864.3	383.15	859.0	393.15	853.6		
70	353.15	880.6	363.15	874.9	373.15	869.8	383.15	864.4	393.15	859.5		
80	353.15	885.4	363.15	880.0	373.15	875.0	383.15	870.0	393.15	864.9		
90	353.15	890.3	363.15	884.9	373.15	879.8	383.15	874.7	393.15	870.1		
100	353.15	894.7	363.15	889.5	373.15	884.8	383.15	879.9	393.15	875.0		
120	353.15	903.2	363.15	898.2	373.15	893.4	383.15	888.7	393.15	884.2		
140	353.15	911.0	363.15	906.2	373.15	901.5	383.15	896.9	393.15	892.5		
160	353.15	918.3	363.15	913.6	373.15	909.1	383.15	904.6	393.15	900.4		
180	353.15	925.3	363.15	920.7	373.15	916.2	383.15	911.8	393.15	907.7		
200	353.15	931.8	363.15	927.3	373.15	922.9	383.15	918.7	393.15	914.6		

[a] Standard uncertainties u are u(T) = 0.1 K, u(p) = 0.01 MPa and the combined expanded uncertainties U (level of confidence = 0.95) are $U(\rho) = 0.001\ \rho$ up to 100 MPa and $U(\rho) = 0.002\ \rho$between (100 and 200) MPa.

sound of biodiesels up to 200 MPa based only on the composition of fatty acid methyl esters in biodiesels. In this method, the thermophysical properties of a biodiesel are determined based on the properties of the individual fatty acid methyl esters using the following linear combinations that involve v the molar volume and cM_γ the product of speed of sound and molecular weight raised to the power $\gamma = 0.975$ instead of the density and speed of sound respectively:

$$v_{Bio\_Cor} = \sum_i x_i v_{cor,i} \tag{10}$$

$$cM_{\gamma,Bio\_Cor} = \sum_i x_i cM_{\gamma,cor,i} \tag{11}$$

$$\kappa_{T,Bio\_Cor} = \sum_i \phi_i \kappa_{T,cor,i} \tag{12}$$

In these expressions, the weigh x_i correspond to the mole fraction of the *i-th* FAME in the biodiesel whereas $\phi_{cor,i}$ is the volume fraction. It is defined as:

$$\phi_{cor,i} = \frac{x_i \; v_{cor,i}}{\sum_K x_k v_{cor,k}} \tag{13}$$

The volume $v_{cor,i}$ as well as $cM_{\gamma,cor,i}$ of pure components are correlated to pressure p and temperature T using Murnaghan-type equations of state that have the following forms:

$$v_{cor,i} = A_{v,i}\left(1 + B_{v,i}\widetilde{p}\right)^{C_{v,i}} \tag{14}$$

$$cM_{\gamma,cor,i} = A_{cM\gamma,i}\left(1 + B_{cM\gamma,i}\widetilde{p}\right)^{C_{cM\gamma,i}} \tag{15}$$

The compressibility $\kappa_{T,i}$, obtained from derivation of Eq. (14) with respect to pressure, is given by:

$$\kappa_{T,cor,i} = -\frac{B_{v,i}C_{v,i}}{1 + B_{v,i}\widetilde{p}} \tag{16}$$

where $\widetilde{p}$ is the relative pressure: $p - p_{atm}$ and coefficients $A_{v,i}, B_{v,i}, C_{v,i}$ and $A_{cM\gamma,i}, B_{cM\gamma,i}, C_{cM\gamma,i}$ are expressed as a function of temperature by second order polynomials whose coefficients were reported in previous publications [9,11] for each FAME between C10:0 and C24:0.

After calculation of pure component properties $v_i, \kappa_{T,i}$ and $cM_{\gamma,i}$ and application of combining rules given by Eqs. (9)–(11), the density and speed of sound in biodiesel are determined from the following thermodynamic relations:

$$\rho_{Bio\_Cor} = \frac{\sum_i x_i M_i}{v_{Bio\_Cor}} \tag{17}$$

$$c_{Bio\_Cor} = \frac{cM^{1/\gamma}_{\gamma,Bio\_Cor}}{\sum_i x_i M_i} \tag{18}$$

where as the isentropic compressibility κ_{S,Bio_Cor} and acoustic impedance Z_{Bio_Cor} of biodiesels are determined from Eqs. (8) and (9) in the same way as for the experimental data.

To evaluate the accuracy of the model, the predicted values were compared with the experimental measurements for all the investigated properties. This was done by calculating the percentage deviation between the calculated and experimental values. The results of this comparative analysis for both biodiesels are summarized in Table 5 where the *MPD*, *MAPD* and *MaxPD* are given for each property and for each biodiesel. To provide a more comprehensive understanding of the observed percentage deviations, the table also includes the relative expanded uncertainty for each thermophysical property studied. This was obtained by multiplying the maximum combined standard uncertainty by the coverage factor $k = 2$. This additional information can help in interpreting the accuracy of the model's predictions.

Upon analyzing the data presented in Table 5, it can be observed that there is a very good agreement between the predicted values and the

Table 5
Statistical characteristics for the prediction of volumetric and acoustic properties for sunflower biodiesel (MB-SF) and palm + rapeseed + soy blend biodiesel (MB-PRS) between 0.1 and 200 MPa in the temperature range 293.15–393.15 K.

Properties	MB-SF	MB-PRS	*Uexp*				
	MPD	*MAPD*	*MaxPD*	*MPD*	*MAPD*	*MaxPD*	
ρ	−0.27	0.26	0.43	−0.57	0.54	0.71	0.2
c	0.15	0.17	0.49	0.03	0.11	0.44	0.3
κ_T	−1.92	1.86	5.06	0.03	1.20	4.10	4
κ_S	−0.04	0.18	0.65	0.51	0.53	1.16	0.6
z	−0.11	0.13	0.39	−0.54	0.52	0.85	0.4

[a]MPD: Mean Percentage Deviation; *MAPD*: Mean Absolute Percentage Deviation; *MaxPD*: maximum percentage deviation; *Uexp: maximum expended uncertainty* (level of confidence = 0.95) *in experimental measurements*.

experimental data for all the properties tested. The average absolute deviation is of the same order of magnitude as the experimental uncertainty for all properties. The maximum deviation observed is never more than twice the measurement uncertainty. Specifically, the model accurately predicts the speed of sound, which is typically a challenging property to predict using correlations or thermodynamic models that rely on equation of state. It should be noted that the maximum deviation for isothermal compressibility is larger compared to other properties. This is because determining the derivatives at the extremities of the derivation domain is a difficult task, and unfortunately the same remains true for both the model calculation and the experiment. The experiment presents a maximum uncertainty on this property at atmospheric pressure, indicating that the error calculated at this point may not be solely attributed to the model, but may also stem from experimental data.

The analysis indicates that there is no systematic deviation between the model predictions and the experimental data. This is further supported by Figs. 1–5, where the observed deviations for 3 isotherms (293.15, 323.15 and 393.15 K) are plotted against pressure. There is no noticeable degradation in the quality of the predictions as the pressure increases, indicating that the model is robust. The predictions for all the properties remain accurate even at the higher pressure (200 MPa). This

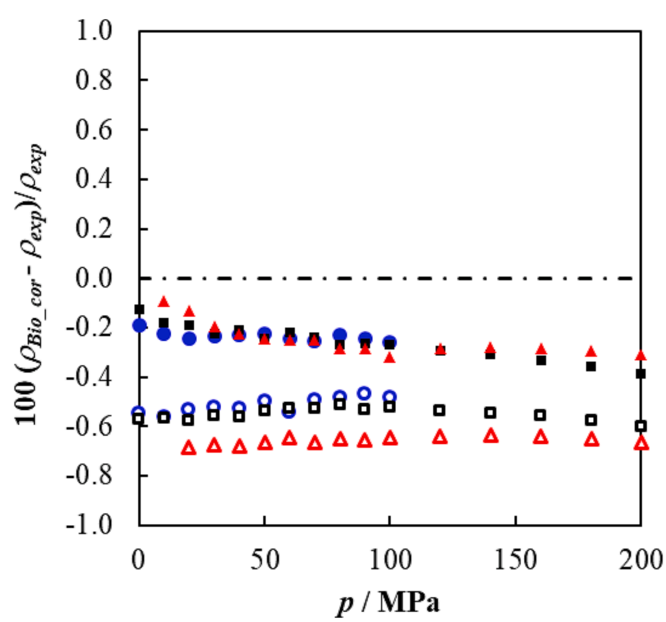

Fig. 1. Relative deviations between the density ρ_{Bio_Cor} calculated using Daridon method [9] and experimental data ρ_{exp} for sunflower methyl biodiesel (MB-SF, represented by solid symbols) and palm + rapeseed + soy methyl biodiesels blend (MB-PRS, represented by hollow symbols) as a function of pressure for three isotherms: ●○, T = 293.15 K; ■□, T = 323.15 K; ▲△, T = 393.15 K.

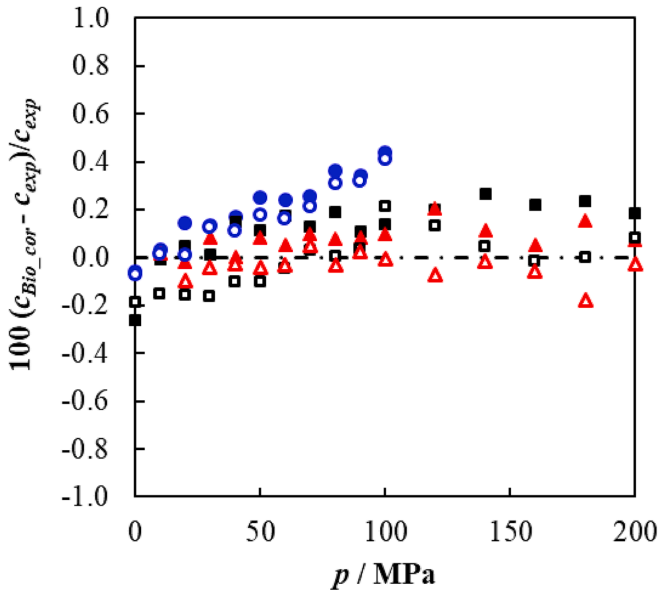

Fig. 2. Relative deviations between the speed of sound c_{Bio_Cor} calculated using Daridon method [11] and experimental data c_{exp} for sunflower methyl biodiesel (MB-SF, represented by solid symbols) and palm + rapeseed + soy methyl biodiesels blend (MB-PRS, represented by hollow symbols) as a function of pressure for three isotherms: ●○, T = 293.15 K; ■□, T = 323.15 K; ▲△, T = 393.15 K.

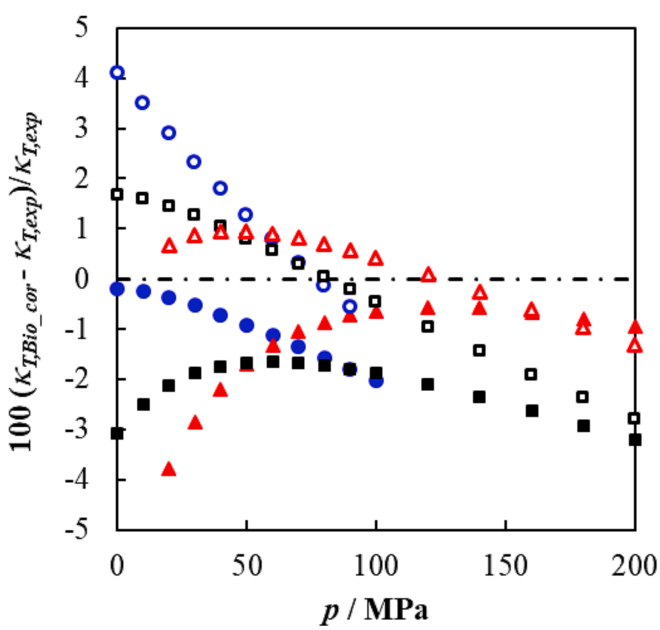

Fig. 3. Relative deviations between the isothermal compressibility κ_{T,Bio_Cor} calculated using Daridon method [9] and experimental data $\kappa_{T,exp}$ for sunflower methyl biodiesel (MB-SF, represented by solid symbols) and palm + rapeseed + soy methyl biodiesels blend (MB-PRS, represented by hollow symbols) as a function of pressure for three isotherms: ●○, T = 293.15 K; ■□, T = 323.15 K; ▲△, T = 393.15 K.

result confirms the earlier tests conducted on two biodiesels (soya and rapeseed) for density and speed of sound at very high pressures. Furthermore, the tests carried out in this study indicate that the good results obtained by the model for density and speed of sound extend to related acoustic properties, such as isentropic compressibility and acoustic impedance.

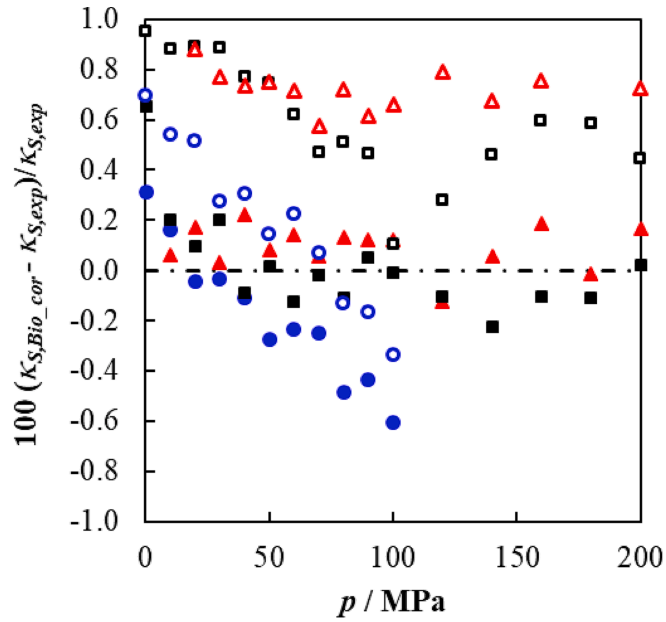

Fig. 4. Relative deviations between the isentropic compressibility κ_{S,Bio_Cor} calculated using Daridon method [9,11] and experimental data $\kappa_{S,exp}$ for sunflower methyl biodiesel (MB-SF, represented by solid symbols) and palm + rapeseed + soy methyl biodiesels blend (MB-PRS, represented by hollow symbols) as a function of pressure for three isotherms: ●○, T = 293.15 K; ■□, T = 323.15 K; ▲△, T = 393.15 K.

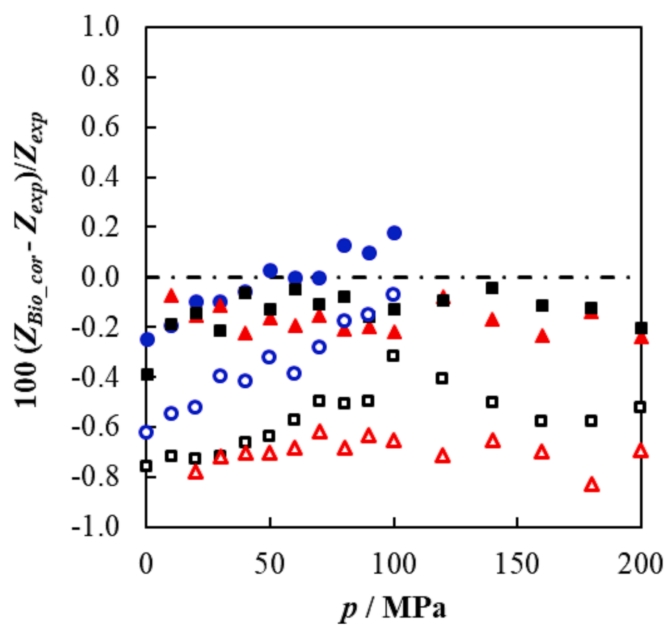

Fig. 5. Relative deviations between the acoustic impedance Z_{Bio_Cor} calculated using Daridon method [9,11] and experimental data Z_{exp} for sunflower methyl biodiesel (MB-SF, represented by solid symbols) and palm + rapeseed + soy methyl biodiesels blend (MB-PRS, represented by hollow symbols) as a function of pressure for three isotherms: ●○, T = 293.15 K; ■□, T = 323.15 K; ▲△, T = 393.15 K.

4. Conclusion

In order to expand the database on the volumetric and acoustic properties of biodiesels within a pressure range compatible with current diesel engine injection conditions, sound density and velocity measures were taken on two biodiesels under high pressure. The first biodiesel was derived from the transesterification of sunflower oil with methanol, while the second was a biodiesel blend of palm, rapeseed, and soybean oil sources. Using a pulsed echo technique operating at 3 MHz, the speed of sound was measured across the full pressure range from 0.1 to 200 MPa. Density values were measured between atmospheric pressure and 100 MPa with a U-shaped vibrating tube densimeter, and between 100 and 200 MPa by integrating the relationship between isothermal compressibility and isentropic compressibility derived from sound velocity measurements. The coupling of these two properties obtained under the same pressure and temperature conditions allowed for the determination of derived properties such as isothermal and isentropic compressibilities, as well as acoustic impedance. These derived fuel properties are critical for the design of the injection process in diesel engines.

The experimental data collected for all of these thermophysical properties were compared in the full *p,T* working range to those calculated by models developed to predict the density and speed of sound of biodiesels up to 200 MPa based on their composition in ester only. Very good agreement was observed between the experimental data and the predictions based on a simple combination rule that relates volume v the speed of sound molecular weight product raised at power g of a biodiesel to their pure component values correlated to pressure and temperature by a Murnaghan-type equation [10]. The mean average percentage deviation between calculated and experimental data is always of the same order of the experimental uncertainty.

Experimentally, this work complements a previous study concerning two different biodiesels: soybean and rapeseed, thus providing a considerable set of acoustic and volumetric properties under very high pressure for 4 different biodiesels. On the modeling side, the comparative study carried out here confirms the validity and reliability of the previously developed models, but so far poorly tested under very high pressure due to the lack of data. Finally, the extended comparison to the derived acoustic properties shows that the two models initially developed separately for density and sound speed can be coupled without generating additional uncertainty for the prediction of acoustic derived properties.

CRediT authorship contribution statement

Matthieu Habrioux: Formal analysis, Methodology, Writing – original draft, Writing – review & editing. **Djamel Nasri:** Formal analysis, Methodology, Writing – original draft, Writing – review & editing. **João A.P. Coutinho:** Formal analysis, Methodology, Writing – original draft, Writing – review & editing. **Jean Luc Daridon:** .

Declaration of Competing Interest

The authors declare that they have no known competing financial interests or personal relationships that could have appeared to influence the work reported in this paper.

Data availability

No data was used for the research described in the article.

Acknowledgments

This work was partly developed within the scope of the project CICECO-Aveiro Institute of Materials, UIDB/50011/2020, UIDP/50011/2020 and LA/P/0006/2020, financed by national funds through the FCT/MCTES (PIDDAC).

Appendix A. Supplementary data

Supplementary data to this article can be found online at https://doi.org/10.1016/j.fuel.2023.128677.

References

[1] Wang X, Huang Z, Zhang W, Kuti OA, Nishida K. Effects of ultra-high injection pressure and micro-hole nozzle on flame structure and soot formation of impinging diesel spray. Appl Energy 2011;88(5):1620–8.
[2] Çelıkten İ. An experimental investigation of the effect of the injection pressure on engine performance and exhaust emission in indirect injection diesel engines. Appl Therm Eng 2003;23(16):2051–60.
[3] Monyem A, H. Van Gerpen J. The effect of biodiesel oxidation on engine performance and emissions. Biomass Bioenergy 2001;20(4):317–25.
[4] Simsek S. Effects of biodiesel obtained from Canola, sefflower oils and waste oils on the engine performance and exhaust emissions. Fuel 2020;265:117026.
[5] Redel-Macías MD, Pinzi S, Leiva-Candia DE, Cubero-Atienza AJ, Dorado MP. Influence of fatty acid unsaturation degree over exhaust and noise emissions through biodiesel combustion. Fuel 2013;109:248–55.
[6] Boudy F, Seers P. Impact of physical properties of biodiesel on the injection process in a common-rail direct injection system. Energ Conver Manage 2009;50(12):2905–12.
[7] Boehman AL, Morris D, Szybist J, Esen E. The impact of the bulk modulus of diesel fuels on fuel injection timing. Energy Fuel 2004;18(6):1877–82.
[8] Ramos MJ, Fernández CM, Casas A, Rodríguez L, Pérez Á. Influence of fatty acid composition of raw materials on biodiesel properties. Bioresour Technol 2009;100(1):261–8.
[9] Daridon JL. Predicting the effect of pressure on biodiesel density at pressures of up to 200 MPa based on fatty acid alkyl ester profiles and density values at atmospheric pressure. Fuel 2020;281:118767.
[10] Murnaghan FD. The compressibility of media under extreme pressures. PNAS 1944;30(9):244–7.
[11] Daridon J-L. Predicting speed of sound in fatty acid alkyl esters and biodiesels at high pressure. Ind Eng Chem Res 2022;61(42):15620–30.
[12] Daridon JL. Predicting and correlating speed of sound in long–chain alkanes at high pressure. Int J Thermophys 2022;43:78.
[13] Habrioux M, Freitas SVD, Coutinho JAP, Daridon JL. High pressure density and speed of sound in two biodiesel fuels. J Chem Eng Data 2013;58(12):3392–8.
[14] Schedemann A, Wallek T, Zeymer M, Maly M, Gmehling J. Measurement and correlation of biodiesel densities at pressures up to 130 MPa. Fuel 2013;107:483–92.
[15] Aitbelale R, Chhiti Y, Alaoui FEM, Sahib Eddine A, Muñoz Rujas N, Aguilar F. High-pressure soybean oil biodiesel density: experimental measurements, correlation by Tait equation, and perturbed chain SAFT (PC-SAFT) modeling. J Chem Eng Data 2019;64(9):3994–4004.
[16] Bessières D, Bazile JP, Nguyen Thi Tanh X, García-Cuadrac F, Acien FG. Thermophysical behavior of three algal biodiesels over wide ranges of pressure and temperature. Fuel 2018;233:497–503.
[17] Aitbelale R, Abala I, M'hamdi Alaoui FE, Eddine AS, Munoz Rujas N, Aguilar F. Characterization and determination of thermodynamic properties of waste cooking oil biodiesel: Experimental, correlation and modeling density over a wide temperature range up to 393.15 and pressure up to 140 MPa. Fluid Phase Equilib 2019:49787–96.
[18] British Standards Institution (BSI). BS EN 14214 Automotive Fuels—Fatty Acid Methyl Esters (FAME) for Diesel Engines—Requirements and Test Methods; BSI: London, U.K., 2009.
[19] Ndiaye EHI, Nasri D, Daridon JL. Speed of sound, density, and derivative properties of fatty acid methyl and ethyl esters under high pressure: Methyl caprate and ethyl caprate. J Chem Eng Data 2012;57(10):2667–76.
[20] Marczak W. Water as a standard in the measurements of speed of sound in liquids. J Acoust Soc Am 1997;102(5):2776–9.
[21] Wilson WD. Speed of sound in distilled water as a function of temperature and pressure. J Acoust Soc Am 1959;31(8):1067–72.
[22] Boelhouwer JWM. Sound velocities in and adiabatic compressibilities of liquid alkanes at various temperatures and pressures. Physica 1967;34(3):484–92.
[23] Daridon JL, Lagourette B, Lagrabette A. Acoustic determination of thermodynamic properties of ternary liquid mixtures up to 150 MPa. Phys Chem Liq 1999;37(2):137–60.
[24] Bazile J-P, Nasri D, Daridon J-L. Speed of sound, density, and derivative properties of Tris(2-ethylhexyl) trimellitate under high pressure. J Chem Eng Data 2017;62(5):1708–15.
[25] Taylor BN, Kuyatt CE. Guidelines for Evaluating and Expressing the Uncertainty of NIST Measurement Results. NIST Technical Note 1297. U.S. Department of Commerce: Washington, DC, 1994.
[26] May EF, Tay WJ, Nania M, Aleji A, Al-Ghafri S, Martin Trusler JP. Physical apparatus parameters and model for vibrating tube densimeters at pressures to 140 MPa and temperatures to 473 K. Rev Sci Instrum 2014;85(9):095111.
[27] Wagner W, Pruß A. The IAPWS formulation 1995 for the thermodynamic properties of ordinary water substance for general and scientific use. J Phys Chem Ref Data 2002;31(2):387–535.
[28] Taylor BN, Kuyatt CE. Guidelines for Evaluating and Expressing the Uncertainty of NIST Measurement Results; NIST Technical Note 1297. Washington DC: U.S. Department of Commerce; 1994.
[29] Daridon JL, Lagrabette A, Lagourette B. Speed of sound, density, and compressibilities of heavy synthetic cuts from ultrasonic measurements under pressure. J Chem Thermodyn 1998;30(5):607–23.

[30] Pratas MJ, Oliveira MB, Pastoriza-Gallego MJ, Queimada AJ, Piñeiro MM, Coutinho JAP. High-pressure biodiesel density: experimental measurements, correlation, and cubic-plus-association equation of state (CPA EoS) modeling. Energy Fuels 2011;25(8):3806–14.

[31] Pratas MJ, Freitas SVD, Oliveira MB, Monteiro SC, Lima ÁS, Coutinho JAP. Biodiesel density: experimental measurements and prediction models. Energy Fuels 2011;25(5):2333–40.

[32] Freitas SVD, Paredes MLL, Daridon JL, Lima AS, Coutinho JAP. Measurement and prediction of the speed of sound of biodiesel fuels. Fuel 2013;103:1018–22.